Supporting Information

Ultrafast Zn^{2+} Diffusion and Exceptional Stability in Self-Assembled 2D VS2/Ti3C2TX Heterostructures for Advanced Zinc-Ion Batteries

Rajesh R. Jaiswar,[a¶] Harishchandra S. Nishad,[a¶] Diwakar Singh,[b] Shashikant P. Patole,[c] and Pravin S. Walke*[a]

[a] National Centre for Nanosciences and Nanotechnology, University of Mumbai Mumbai-400098, India.

[b] Department of Metallurgical Engineering and Materials Science, Indian Institute of Technology Bombay, Mumbai-400076, India.

[c] Department of Physics, Khalifa University of Science and Technology, Abu Dhabi-127788, UAE.

*Corresponding author's email:shivshripsw@gmail.com

Authors contributions: ¶These authors contributed equally.

Enclosed:

Equations: S1 & S2
Figures: S1 to S6
Tables: S2 & S2
Video: S1
References: S1 to S9

Braggs law

$$d = n\lambda\, 2\sin\theta \qquad \text{.....S1}$$

where, where ‘d’ is interplanar spacing (Å), ‘n’ is 1 order of diffraction, and ‘θ’ is peak position in radians.

Scherrer equations

$$D = K\lambda\, \beta\cos\theta \qquad \text{……S2}$$

‘D’ is crystallites size (nm), ‘K’ is 0.9 (Scherrer constant), ‘λ’ is 0.15406 nm (wavelength of the x-ray source), ‘b’ is FWHM (Full Width Half Maximum) in radians.

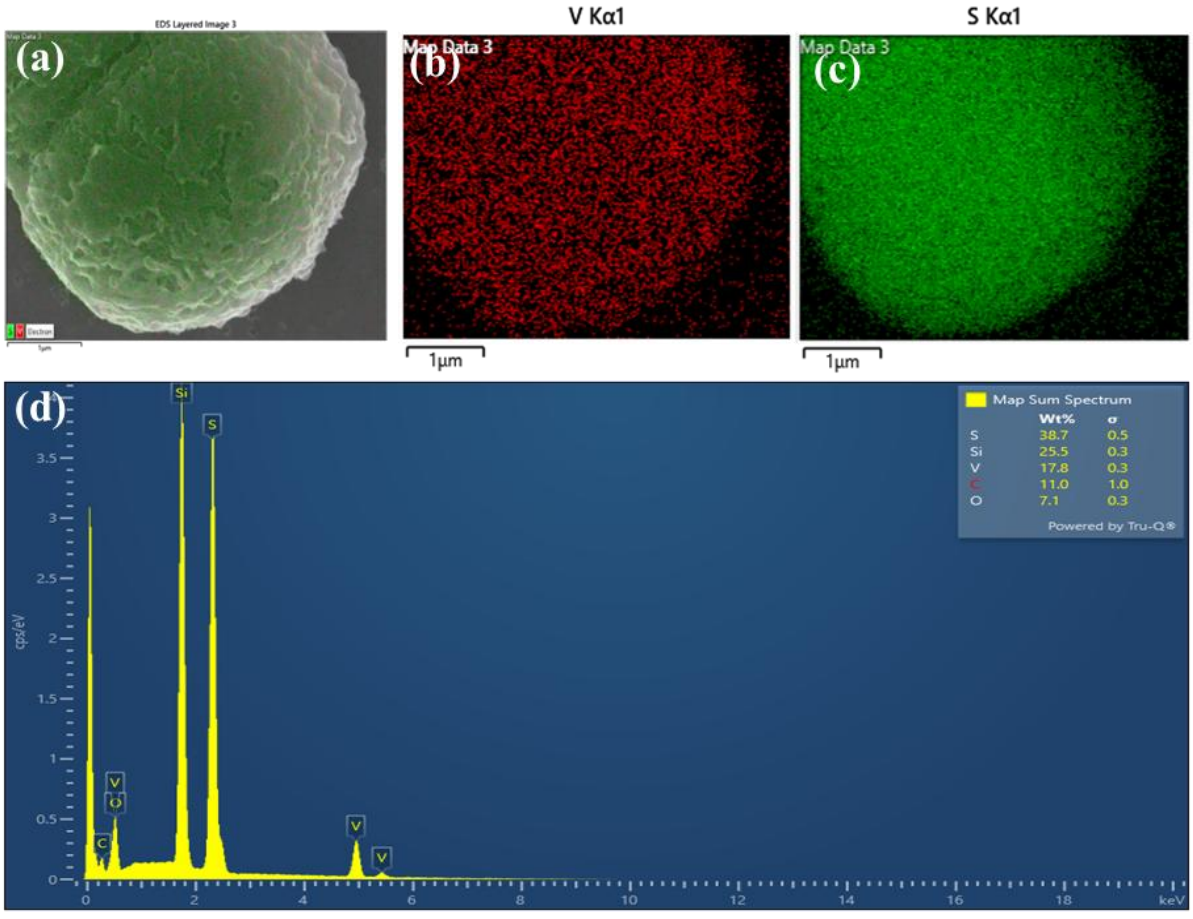

Fig. S1. (a) FESEM image with EDS elemental mapping of V and S, (b, c) Individual elemental mapping of V and S, (d) EDX spectra of VS_2 and inset shows elemental composition.

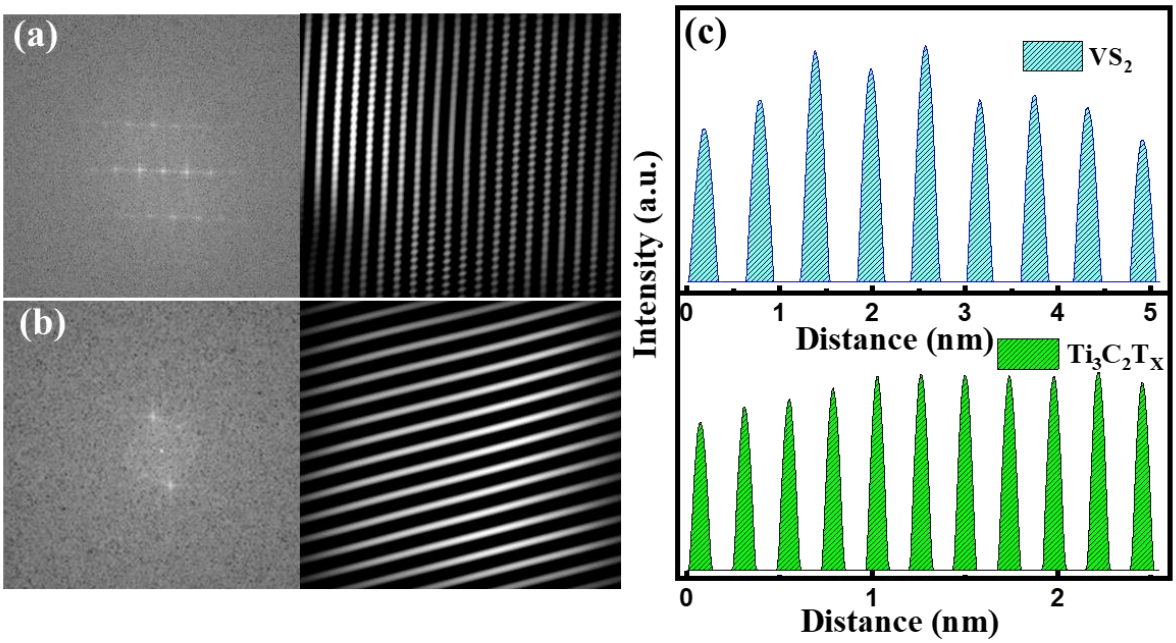

Fig. S2. (a) FFT (left) and IFFT (right) plot of VS_2, (b) FFT (left) and IFTT (right) plot of $Ti_3C_2T_X$, (c) Intensity plot of VS2 (top) and of $Ti_3C_2T_x$ (Bottom).

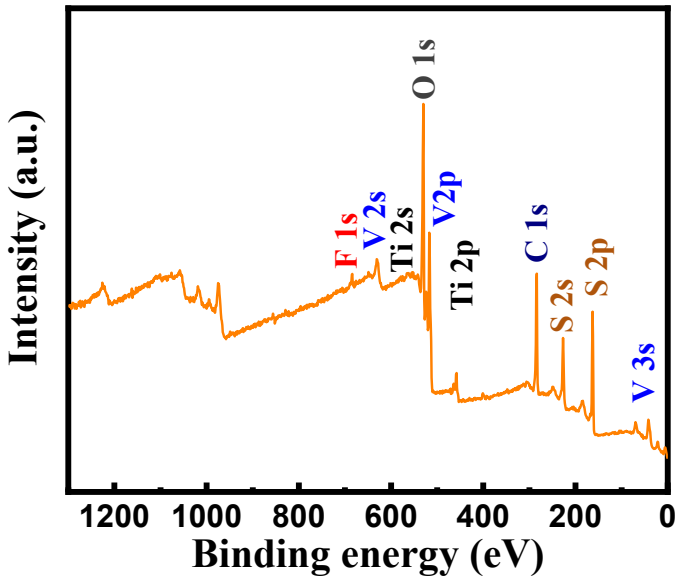

Fig. S3. XPS survey spectrum of the $VS_2/Ti_3C_2T_x$ heterostructure.

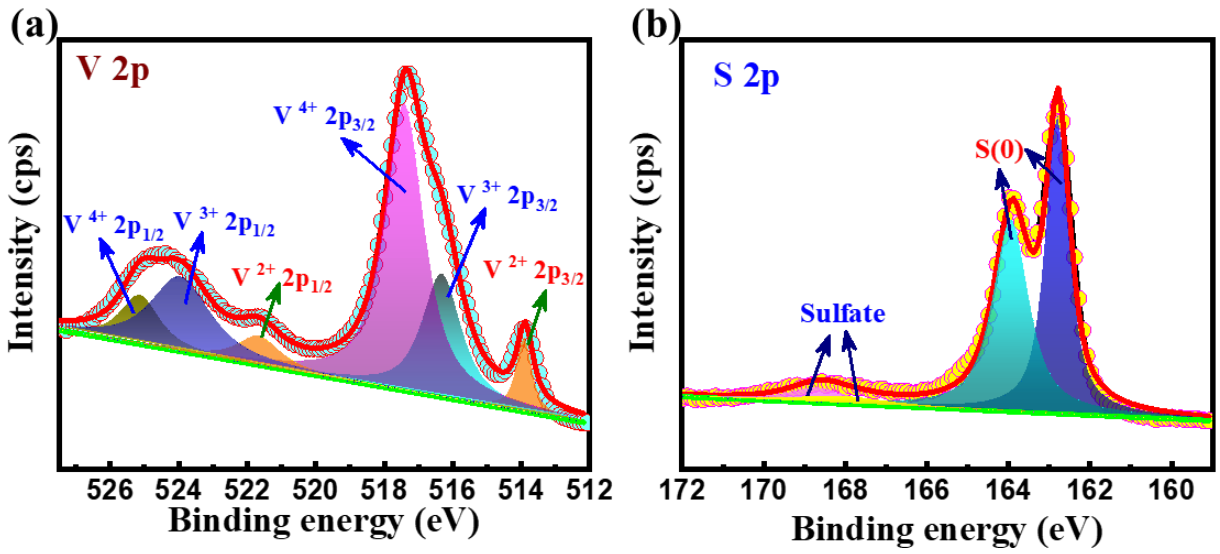

Fig. S4. Deconvoluted XPS spectra of V 2p (a) and S 2p (b) for VS_2.

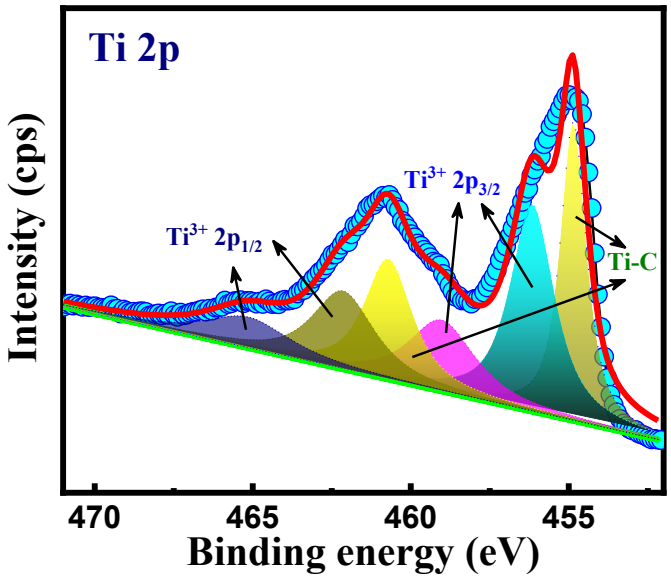

Fig. S5. Deconvoluted XPS spectra Ti 2p spectrum of pristine $Ti_3C_2T_x$.

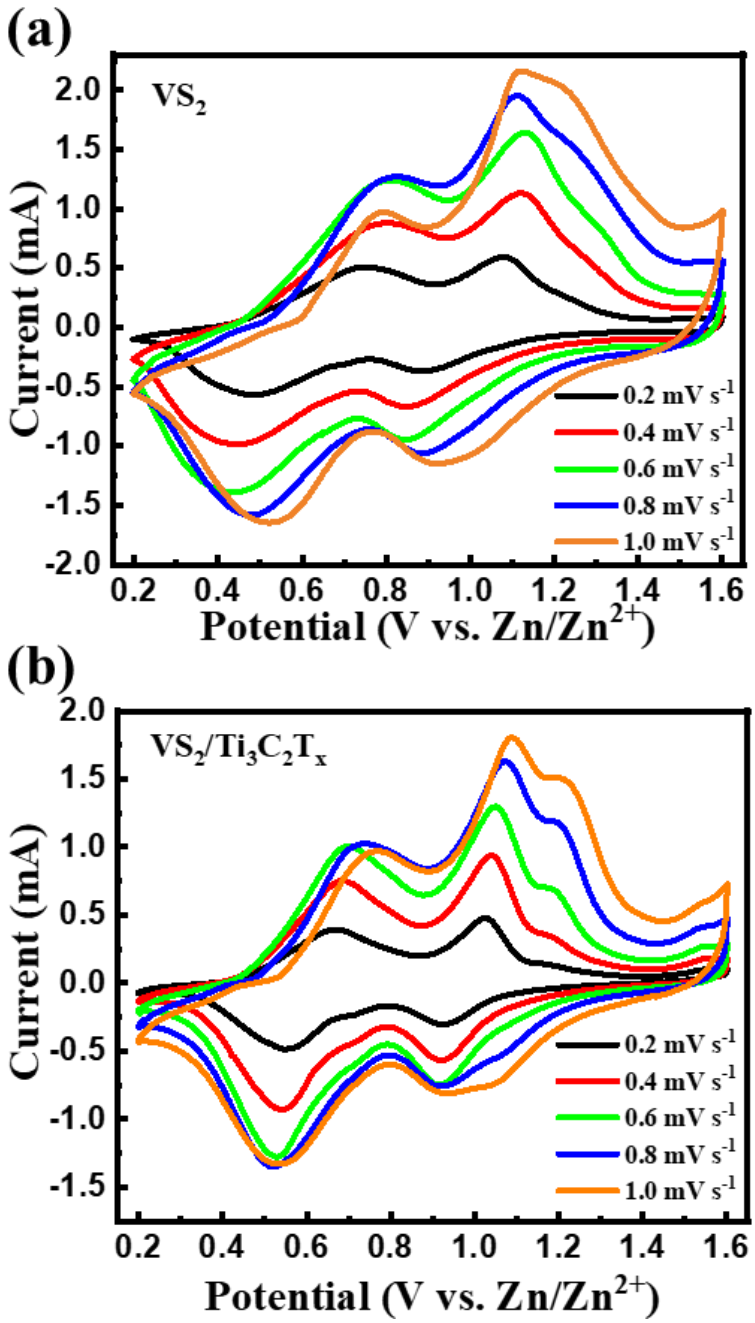

Fig. S6. (a) CV curves of Zn//VS_2 at various scan rates ranging from 0.2 to 1.0 mV s^{-1}, (b) CV curves of Zn// $VS_2/Ti_3C_2T_X$ at various scan rates ranging from 0.2 to 1.0 mV s^{-1}.

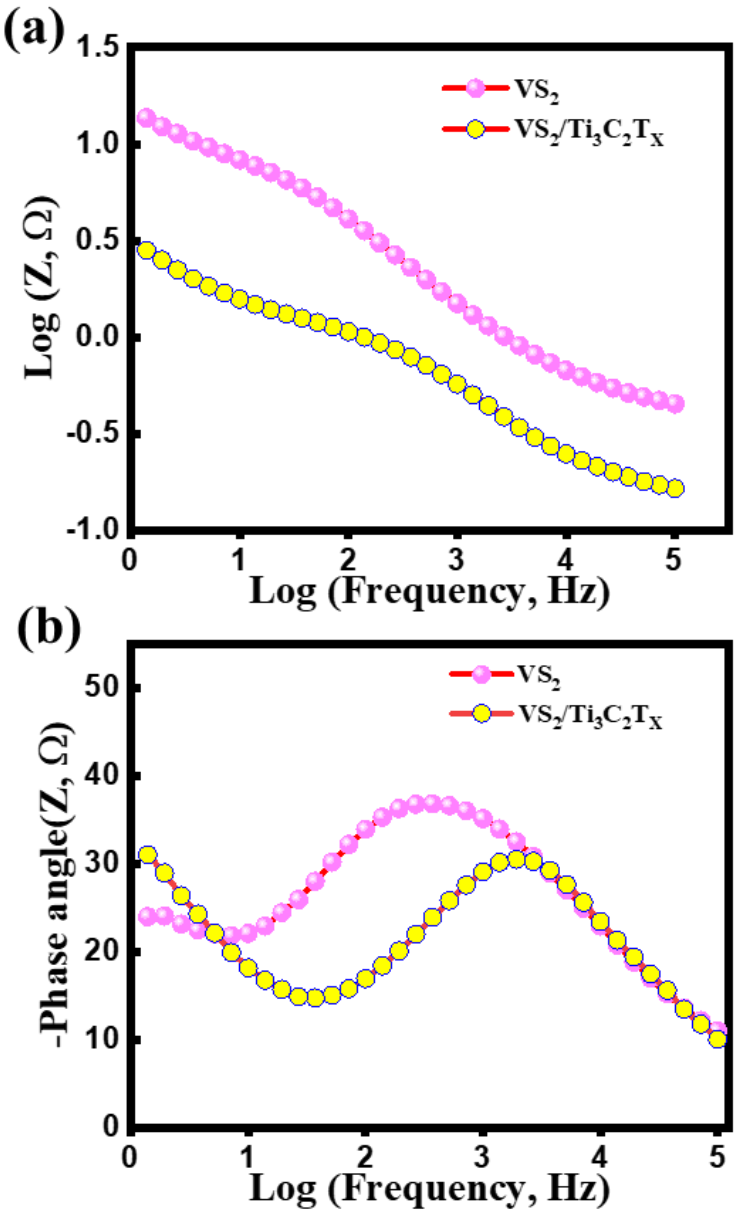

Fig. S7. (a) Bode frequency plot, (b) Bode phase plot.

Table S1. Electrochemical performance of recently reported vanadium sulphide-based cathode materials for aqueous Zn-ion battery.

Sr. No.	Material	Synthesis method	Electrolyte	Specific capacity (mAh g^{-1} @A g^{-1})	Cyclic Stability	Ref.
1.	VS_4@rGO	Hydrothermal	1 M Zn $(CF_3SO_3)_2$	180@1.0	93.3% after 165 cycles at 1.0 A g^{-1}	1
2.	rGO-VS_2	Solvothermal	3 M Zn $(CF_3SO_3)_2$	238@0.1	93% after 1000 cycles at 5.0 A g^{-1}	2
3.	VS_2/VOx	Hydrothermal	25 M $ZnCl_2$	301@0.05	75% after 3000 cycles at 1.0 A g^{-1}	3
4.	VS_2@VOOH	Hydrothermal	3M $ZnSO_4$	184.2@0.05	82% after 400 cycles at 2.5 A g^{-1}	4
5.	$V_{1.11}S_2$	Solvothermal	2M $ZnSO_4$	224.8 at 0.1	130.4 % after 2000 cycles @ 2A g^{-1}	5
6.	VS_4/V_2O_3	CVD	3 M Zn $(CF_3SO_3)_2$	163@0.1	--	6
7.	VS_2@SS	Hydrothermal	1 M $ZnSO_4$	98@0.05	80% after 1600 cycles at 1.0 A g^{-1}	7
8.	VS_2@ SWCNT	Hydrothermal	3 M Zn $(CF_3SO_3)_2$	205.3@0.1	72% after 1500 cycles at 5.0 A g^{-1}	8
9.	VS_2@N-C	Wet chemical	3 M Zn $(CF_3SO_3)_2$	203@0.05	97% after 600 cycles at 1.0 A g^{-1}	9
10.	MOF/MXene	Wet chemical	2 M Zn $(CF_3SO_3)_2$	260.1@0.1	92% after 1000 cycles at 4.0 A g^{-1}	10
11.	VS_2/$Ti_3C_2T_z$	Hydrothermal	1M $ZnSO_4$	285@0.2	74.3 % after 5000 cycles at 2.0 A g^{-1}	11
12.	VS_2/MXene	Hydrothermal	2M $ZnCl_2$-PAM	213.4@0.2	93% after 2400 cycles at 5.0 A g^{-1}	12
13.	**VS_2/$Ti_3C_2T_x$**	**Hydrothermal**	**3 M Zn $(CF_3SO_3)_2$**	**287@0.2**	**95% after 2000 cycle at 5 A g^{-1}**	**This work**

Table S2. Electrochemical impedance spectroscopy (EIS): intrinsic resistance (Rs), charge transfer resistance (R_{CT}), diffusion resistance for Zn//VS_2 and Zn//VS_2/$Ti_3C_2T_x$.

Material	R_S (Ω)	R_{CT} (Ω)	Zw (Ω)
VS_2	0.44	8.59	7.0
VS_2/$Ti_3C_2T_x$	0.16	1.16	1.1

Video S1: The practical application of the VS_2/$Ti_3C_2T_X$ heterostructure cathode was demonstrated by assembling two-coin cells (Zn//VS_2/$Ti_3C_2T_X$) in a series, which was charged for 15 seconds. These cells successfully powered 40 commercial LEDs (1.8 V) and glowing LED's for almost 3 minutes. It demonstrated fast charging capacity with long time working.

References

1 H. Qin, Z. Yang, L. Chen, X. Chen and L. Wang, *J. Mater. Chem. A*, 2018, **6**, 23757–23765.

2 T. Chen, X. Zhu, X. Chen, Q. Zhang, Y. Li, W. Peng, F. Zhang and X. Fan, *J. Power Sources*, 2020, **477**, 228652.

3 D. Yu, Z. Wei, X. Zhang, Y. Zeng, C. Wang, G. Chen, Z. X. Shen and F. Du, *Adv. Funct. Mater.*, 2021, **31**, 2008743.

4 J. Xu, Y. Liu, P. Chen, A. Wang, K. Huang, L. Fang and X. Wu, *J. Colloid Interface Sci.*, 2022, **620**, 119–126.

5 X. Chen, Q. Kong, X. Wu, X. An, J. Zhang, Q. Wang and W. Yao, *J. Colloid Interface Sci.*, 2022, **625**, 1002–1011.

6 J. Ding, H. Gao, W. Liu, S. Wang, S. Wu, S. Fang and F. Cheng, *J. Mater. Chem. A*, 2021, **9**, 11433–11441.

7 T. Jiao, Q. Yang, S. Wu, Z. Wang, D. Chen, D. Shen, B. Liu, J. Cheng, H. Li, L. Ma, C. Zhi and W. Zhang, *J. Mater. Chem. A*, 2019, **7**, 16330–16338.

8 H. Sun, L. Yang, E. Hu, M. Feng, C. Fan, W. Wang, H. Li, X. Wang and Z. Liu, *ACS Appl. Mater. Interfaces*, 2022, **14**, 40247–40256.

9 J. Liu, W. Peng, Y. Li, F. Zhang and X. Fan, *J. Mater. Chem. C*, 2021, **9**, 6308–6315.

10 Y. Wang, J. Song and W.-Y. Wong, *Angew. Chemie Int. Ed.*, 2023, **62**, e202218343.

11 L. Zhang, Y. Li, X. Liu, R. Yang, J. Qiu, J. Xu, B. Lu, J. Rosen, L. Qin and J. Jiang, *Adv. Sci.*, 2024, **11**, 2401252.

12 Y. Feng, Y. Feng, Y. Zhang, L. Sun, X. Li, M. Meng, Y. Zhu and K. Liu, *J. Power Sources*, 2022, **545**, 231944.